Relationships between geomechanical properties and lithotypes in NW European chalks

FANNY DESCAMPS[1]*, OPHÉLIE FAŸ-GOMORD[2], SARA VANDYCKE[1], CHRISTIAN SCHROEDER[3], RUDY SWENNEN[2] & JEAN-PIERRE TSHIBANGU[1]

[1]*UMONS, University of Mons, 20 place du Parc, 7000 Mons, Belgium*

[2]*Department of Earth and Environmental Sciences, KU Leuven, Katholieke Universiteit Leuven, Geology, Celestijnenlaan 200E, 3001 Heverlee, Belgium*

[3]*ULB, Université Libre de Bruxelles, 50 avenue Roosevelt, 1050 Brussels, Belgium*

**Correspondence: fanny.descamps@umons.ac.be*

Abstract: As a result of increasing interest in unconventional reservoirs, a wide range of sedimentary systems are now being investigated with regard to petroleum applications, including various tight chalk formations. We examined a wide variety of chalk samples from NW Europe (micritic, grainy, argillaceous, marl seam, cemented and silicified chalks) and investigated the relationships between their petrophysical properties, mechanical properties and associated microtextures and how diagenesis can affect these properties. A diagenesis index based on an evaluation of textural and diagenetic parameters was used to quantify the effect of global porosity-reducing diagenesis on the microtexture of chalks. We used petrographic and petrophysical measurements to determine the petrography, density, porosity, permeability and sonic velocity of the chalk samples and uniaxial compression experiments to assess their mechanical behaviour. Our dataset of >30 samples covers a wide range of values for these properties. We determined a linear porosity–permeability relationship controlled by the diagenesis index. Porosity influences the unconfined compressive strength and Young's modulus, but our analyses suggest that the diagenesis of the studied lithologies provides us with a further understanding of the mechanical behaviour of chalks. Micritic and grainy chalks are associated with the lowest diagenesis index and exhibit the lowest strength, whereas the higher diagenesis indices observed for other microtextures correspond to higher compressive strengths.

High-porosity pure white chalks have been extensively studied in relation to oil and gas production for >40 years (e.g. Schroeder 1995, 2002; Delage *et al.* 1996; Papamichos *et al.* 1997; Homand *et al.* 1998; Risnes & Flaageng 1999; Homand & Shao 2000*a*, *b*, *c*; Gommesen & Fabricius 2001; Risnes 2001; Collin *et al.* 2002; DeGennaro *et al.* 2003, 2005; Risnes *et al.* 2003; Nguyen *et al.* 2008). Recently, however, there has been increasing interest in unconventional reservoirs, such as tight chalk formations, leading to a need to investigate a wider range of sedimentary and diagenetic systems.

Several studies have focused on the characterization of microtextures and pore networks within microporous carbonate reservoirs (Cantrell & Hagerty 1999; Richard *et al.* 2005; Vincent *et al.* 2011; Brigaud *et al.* 2014; Regnet *et al.* 2014; Kaczmarek *et al.* 2015). Classifications based on the morphology of the micritic matrix have been developed for microcrystalline calcite (Lambert *et al.* 2006; Deville de Periere *et al.* 2011; Kaczmarek *et al.* 2015). However, the proposed classifications are not applicable to chalk because they do not include the nanobioclast component. Mortimore & Fielding (1990) attempted to classify chalk microtextures based on scanning electron microscopy (SEM) observations, with a classification applicable to pure chalks only.

Fritsen *et al.* (1996) proposed a classification of chalks based on macroscopic observations from North Sea cores. Mallon & Swarbrick (2002, 2008) focused on the petrographic and petrophysical properties of non-reservoir low-permeability chalk lithologies. These deposits were defined by the Joint Chalk Research (JCR) group (Bailey *et al.* 1999) as tight chalks and include all chalks with a matrix permeability <0.2 mD. They are of interest to the petroleum industry (Fabricius 2001; Røgen & Fabricius 2002; Strand *et al.* 2007; Lindgreen & Jakobsen 2012) because they might be underexplored reservoirs or may have a crucial role in hydrocarbon migration, acting as seals or fluid conduits depending on their fracture pattern (Gennaro *et al.* 2013).

Depositional and diagenetic processes are known to control chalk microtextures (Anderskouv

From: Turner, J. P., Healy, D., Hillis, R. R. & Welch, M. J. (eds) *Geomechanics and Geology*. Geological Society, London, Special Publications, **458**, https://doi.org/10.1144/SP458.9

& Surlyk 2011). The size and connectivity of the pore network may be enhanced by dissolution or reduced by cementation and compaction. Hence microtexture appears to be the link between the current behaviour of chalk formations and their geological history. Rashid *et al.* (2015) examined the factors affecting the distribution of porosity, permeability and reservoir quality in the Kometan Formation (northern Iraq). Faÿ-Gomord *et al.* (2016*a*) proposed an in-depth understanding of the microtexture of tight chalks and highlighted the controlling role of the non-carbonate content and the degree of diagenesis on the petrophysical properties.

Few studies are currently available on the mechanical properties of tight chalks. This is, however, essential for designing hydraulic fracturing in tight formations, such as the Niobrara plays in the USA, where diagenetic changes have been proved to increase the brittleness of chalk (Pollastro 2010; Maldonado *et al.* 2011). Bell *et al.* (1999) reviewed the engineering properties of English chalk, including some tight chalks. Using indentation experiments, Faÿ-Gomord *et al.* (2016*b*) highlighted the role of microtextures in the mechanical behaviour of chalk and underlined the distinct behaviour of tight chalk.

The study reported here investigated how diagenesis can affect the petrophysical and mechanical properties of chalk by studying the relationships between these properties and the associated microtextures. This will help our understanding of the behaviour of tight chalk formations in terms of storage capacity, transport mechanisms and mechanical behaviour. It is also of interest when searching for good analogues from outcrops because diagenesis has proved to be a key issue for the characterization of reservoir chalk from chalk outcrops (Hjuler & Fabricius 2009).

Sample areas

NW European chalks were investigated from several outcrops in Belgium, France and the UK (Fig. 1). The Belgian samples were from the Harmignies quarry, where pure white chalks from the Mons Basin are exploited. The samples came from the following Campanian formations (Marlière 1949):

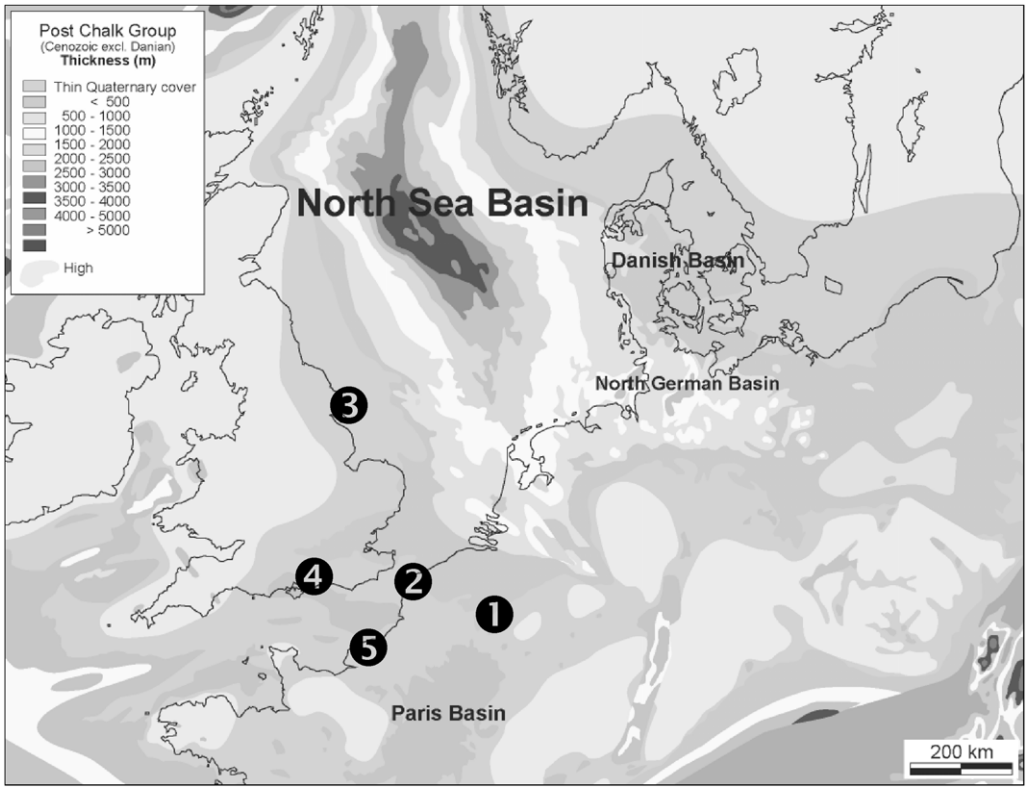

Fig. 1. Location of outcrop samples (modified from Hjuler & Fabricius 2009). 1, Harmignies Quarry (Belgium); 2, Boulonnais (France); 3, Yorkshire (UK); 4, Sussex (UK); and 5, Upper Normandy (France).

Obourg (CH01), Nouvelles (CH02) and Spiennes (CH03). In Belgium, Campanian pure white chalk is exploited in different quarries in the Mons Basin and in the East Chalk district near Lixhe village (Robaszynski *et al.* 2001). These pure white chalks contain a majority of intact coccoliths and are considered as analogous to chalk reservoirs; they have been extensively studied (Schroeder 2002; Papamichos *et al.* 2012; Megawati *et al.* 2015). The Belgian white chalk is affected by normal and strike-slip faulting with a large number of major joints (Vandycke *et al.* 1991; Vandycke 2002).

In France, outcrops were studied in the Boulonnais region (Cap Blanc Nez site) and in Upper Normandy at different locations along the coast in Cenomanian to Turonian chalks (Table 1). The Cenomanian deposits of Cap Blanc Nez have been described as evolving from silicate-rich chalk in the Lower Cenomanian towards white chalk at the top (Robaszynski & Amédro 1986; Amédro & Robaszynski 2001). The argillaceous chalk is related to a strong detrital input, most probably from the Brabant Massif (Deconinck *et al.* 1991); the input decreased as the depositional environment deepened during the Late Cretaceous. The Normandy Basin is well known and has been well studied (Juignet 1974; Kennedy & Juignet 1975; Quine & Bosence 1991; Mortimore & Pomerol 1997; Robaszynski *et al.* 1998; Lasseur *et al.* 2009).

Samples were taken from two sites in the British chalk district. The Flamborough Head samples are clean Santonian chalk (Whitham 1993), which has been deeply buried (Menpes & Hillis 1996) and has thus undergone strong burial diagenesis (Faÿ-Gomord *et al.* 2016*a*). The samples from Sussex (southern England) were only buried by up to 700 m (Law 1998). Several formations display very different lithotypes, from clean chalk with flint bands in the Birling Gap Turonian New Pit Formation, to argillaceous Cenomanian chalk from Eastbourne.

This first overview of sampling sites (Table 1; Fig. 1) shows the wide variety of chalk materials considered in this study. Their selection was governed by our search for a diversity of lithotypes and geological burial histories. Samples were also specifically selected in zones that were not influenced by faults (Gaviglio *et al.* 2009). As indicated on Figure 1, the chalk formations represent different burial depths, ranging from 200 to 250 m for the Harmignies chalk (Dupuis & Vandycke 1989) to >1200 m for the Flamborough Head chalk (Menpes & Hillis 1996). This study focused on chalks already referenced in terms of lithostratigraphy (Table 1) for all the different sites. Some of the mechanical properties are currently known, but no clear relationship has been established between the diagenetic features and mechanical properties.

Methodology

Petrographic analysis: development of a diagenesis index

Classification systems for chalk microtextures and the degree of diagenesis are often subjective. To develop a quantitative approach allowing comparison with other properties, the microtexture and diagenesis need to be assessed using a numerical value. This will establish a key link between the geology and the petrophysical and geomechanical properties.

We obtained microphotographs from careful SEM observations of the samples to document the microtextures at different magnifications. The diagenesis index, developed by Faÿ-Gomord *et al.* (2016*a*), was assessed for each sample. This index is based on seven diagenetic criteria, which are each graded from 0 (low diagenesis) to 10 (intense diagenesis); the average value, calculated from the seven grades for each studied sample, determines the diagenesis index (Fig. 2). The seven diagenetic criteria are: (1) the micritic microtexture; (2) grain contacts; (3) coccolith disintegration; (4) cemented zones; (5) authigenic calcite crystals; (6) coccolith grain overgrowth; and (7) intraparticle cement. Figure 3 shows typical micrographs corresponding to extreme cases encountered for each of the criteria assessed in the diagenesis index. Each criterion is described below.

Micritic microtexture. The micritic microtexture corresponds to the general arrangement of particles in the matrix. The micritic fraction is defined as particles <10 μm. The microtexture can be loose (with a grading 0–3), tight (4–7) or anhedral compact (8–10). A similar classification was used by Lambert *et al.* (2006) and Deville de Periere *et al.* (2011). The micritic microtexture is often closely related to compaction because the arrangement of grains depends on both mechanical and chemical compaction during burial diagenesis. However, the arrangement of grains that affects the overall microtexture can also be affected by eogenesis during early lithification, as is seen with hardgrounds.

Grain contacts. The types of contact between micritic particles range from punctic contacts (0–2), serrate contacts (3–4), meshed contacts (5–6), coalescent contacts (7–8) to fused contacts (9–10). A punctic contact means that the contacts between grains are punctual and the grains seem to only lie on each other. A serrate contact refers to adjoined grains, connected to each other by a surface. A meshed contact occurs when the grains show indentation of adjacent grains; they are partly nested together. A coalescent contact refers to grains that

Table 1. *Geographical and stratigraphic location of the samples*

Sample no.	Sampling site	Formation	Stratigraphy	Lithotype	References*
CH01	Harmignies Quarry, Belgium	Obourg	Middle Campanian	Micritic	3, 10
CH02	Harmignies Quarry, Belgium	Nouvelles	Middle Campanian	Micritic	3, 10
CH04	Harmignies Quarry, Belgium	Spiennes	Upper Campanian	Micritic	3, 10
CO01	Coquelles Quarry, Boulonnais, France	Caffier	Santonian	Micritic	1, 14
NH03	Newhaven. Sussex, UK	Newhaven	Campanian	Micritic	4, 8, 12, 13
RA01	Ramsgate. Kent, UK	Seaford	Santonian	Micritic	4, 8, 12, 13
BG01	Birling Gap. Sussex, UK	New Pit	Turonian	Grainy	4, 8, 12, 13
CM02	Mimoyecques Quarry. Boulonnais, France	Guet	Turonian	Grainy	1
CM06	Mimoyecques Quarry. Boulonnais. France	Guet	Turonian	Grainy	1
ETR33	Etretat, Upper Normandy, France	Saint Pierre en Port	Coniacian	Grainy	7, 9, 12, 15
SS01	Seven Sisters, Sussex, UK	Chalk mudstone	Coniacian	Grainy	4, 8, 12, 13
CB14	Cap Blanc Nez, Boulonnais, France	Escalles	Upper Cenomanian	Cemented	2, 6, 14
FA15	Flamborough Head, Yorkshire, UK	Flamborough	Santonian	Cemented	10, 16
FA39B	Flamborough Head, Yorkshire, UK	Flamborough	Santonian	Cemented	10, 16
FH11	Flamborough Head, Yorkshire, UK	Flamborough	Santonian	Cemented	10, 16
SC01	Saint Martin en Campagne, Upper Normandy, France	Tilleul	Turonian	Cemented	7, 9, 12, 15
CB13	Cap Blanc Nez, Boulonnais, France	Escalles	Upper Cenomanian	Marl seams	2, 6, 14
CB16	Cap Blanc Nez, Boulonnais, France	Grand Nez	Base Turonian	Marl seams	2, 6, 14
EA02	Eastbourne. Sussex, UK	Hollywell Nodular	Base Turonian	Marl seams	4, 5, 8, 12, 13
ETR21	Senneville, Upper Normandy, France	Senneville	Middle Turonian	Marl seams	7, 9, 12, 15
ETR47	Senneville, Upper Normandy, France	Senneville	Middle Turonian	Marl seams	7, 9, 12, 15
SC02	Saint Martin en Campagne, Upper Normandy, France	Tilleul	Turonian	Marl seams	7, 9, 12, 15
SC03	Saint Martin en Campagne, Upper Normandy, France	Tilleul	Turonian	Marl seams	7, 9, 12, 15
CB02	Cap Blanc Nez, Boulonnais, France	Strouanne	Lower Cenomanian	Argillaceous	2, 6, 14
CB04	Cap Blanc Nez, Boulonnais, France	Strouanne	Lower Cenomanian	Argillaceous	2, 6, 14
CB06	Cap Blanc Nez, Boulonnais, France	Strouanne	Lower Cenomanian	Argillaceous	2, 6, 14
CB07	Cap Blanc Nez, Boulonnais, France	Petit Blanc-Nez	Lower Cenomanian	Argillaceous	2, 6, 14
CB09	Cap Blanc Nez, Boulonnais, France	Petit Blanc-Nez	Mid-Cenomanian	Argillaceous	2, 6, 14
CB10	Cap Blanc Nez, Boulonnais, France	Petit Blanc-Nez	Mid-Cenomanian	Argillaceous	2, 6, 14

(*Continued*)

Table 1. (*Continued*)

Sample no.	Sampling site	Formation	Stratigraphy	Lithotype	References*
CB11	Cap Blanc Nez, Boulonnais, France	Cran	Mid-Cenomanian	Argillaceous	2, 6, 14
CB23	Cap Blanc Nez, Boulonnais, France	Petit Blanc-Nez	Lower Cenomanian	Argillaceous	2, 6, 14
CB24	Cap Blanc Nez, Boulonnais, France	Petit Blanc-Nez	Lower Cenomanian	Argillaceous	2, 6, 14
CB25	Cap Blanc Nez, Boulonnais. France	Petit Blanc-Nez	Lower Cenomanian	Argillaceous	2, 6, 14
EA01	Eastbourne. Sussex, UK	Zig-Zag	Cenomanian	Argillaceous	4, 5, 8, 12, 13
BR01	Bruneval, Upper Normandy, France	Glauconieuse	Cenomanian	Silicified	7, 9, 12, 15

*Studies performing geological logs on the studied outcrops: (1) Amédro & Robaszynski (2000); (2) Amédro & Robaszynski (2001); (3) Boulvain & Pingot (2012); (4) Bristow *et al.* (1997); (5) Gale *et al.* (2005); (6) Gräfe (1999); (7) Juignet (1974); (8) Kennedy (1969); (9) Lasseur *et al.* (2009); (10) Marlière (1949); (11) Mitchell (1994); (12) Mortimore & Pomerol (1997); (13) Mortimore (2011); (14) Robaszynski & Amédro (1986); (15) Robaszynski *et al.* (1998); (16) Whitham (1993). From Faÿ-Gomord *et al.* (2016*a*, *b*).

are difficult to identify because several grains are nested together. A fused contact corresponds to a contact where it is impossible to define clearly the boundaries of the grains. The contact between grains depends on both mechanical compaction and pressure dissolution, particularly grain-to-grain contact dissolution processes, which are often enhanced in the presence of clays.

Coccolith disintegration. When sediments are buried, gravitational forces induce mechanical compaction. The grains are brought closer together and the mechanical breakage of delicate coccolith tests increases as the overburden pressure increases. The crushing of microfossils requires stress levels corresponding to significant depths, even if some species break more easily than others, depending on the thickness of their tests. This evidence of burial diagenesis can be graded from 0, when all the coccoliths are well preserved, to 10, when the coccolith tests are broken apart into very small – sometimes hardly recognizable – tests.

Cemented zones. The cemented zones are defined as homogeneous surfaces of calcite cement for which the longest surface trace observed on the micrograph is >10 μm. These zones result from calcite cementation either during eogenesis (hardgrounds) or burial diagenesis. This criterion is ranked from 0, when cemented zones are absent, to 10 when they represent at least 50% of the chalk sample.

Authigenic calcite crystals. Authigenic calcite crystals generally occur as euhedral crystals of apparently non-biogenic origin, usually measuring 1–5 μm. These authigenic crystals have previously been reported as associated with both early diagenetic processes (Faÿ-Gomord *et al.* 2016*a*) and burial diagenesis (Fabricius 2003). This criterion is rated from 0 (no authigenic crystals) to 10 (a high density of authigenic crystals).

Coccolith grain overgrowth. Coccolith fragments often exhibit calcite cement overgrowths, but the degree of occurrence is significantly variable. This diagenetic criterion ranges from 0 for none to very few overgrowth cements, to 10 when almost all the nanofossils show overgrowths. Cement overgrowth results from the dissolution of calcite from less stable surfaces and reprecipitation on stable

Criteria	From	1 10	To	Mark
Micritic matrix texture	Microrhombic		Anhedral	7
Grain contact	Punctic		Coalescent	3
Coccolith disintegration	Low		High	6
Cemented zone	Absent		Common	7
Automorphous cement	Absent		Common	5
Coccolith grain overgrowth	Absent		Common	5
Intraparticle cementation	Absent		Common	3
			TOTAL	5

Fig. 2. Example of diagenesis index assessment from the evaluation of seven criteria.

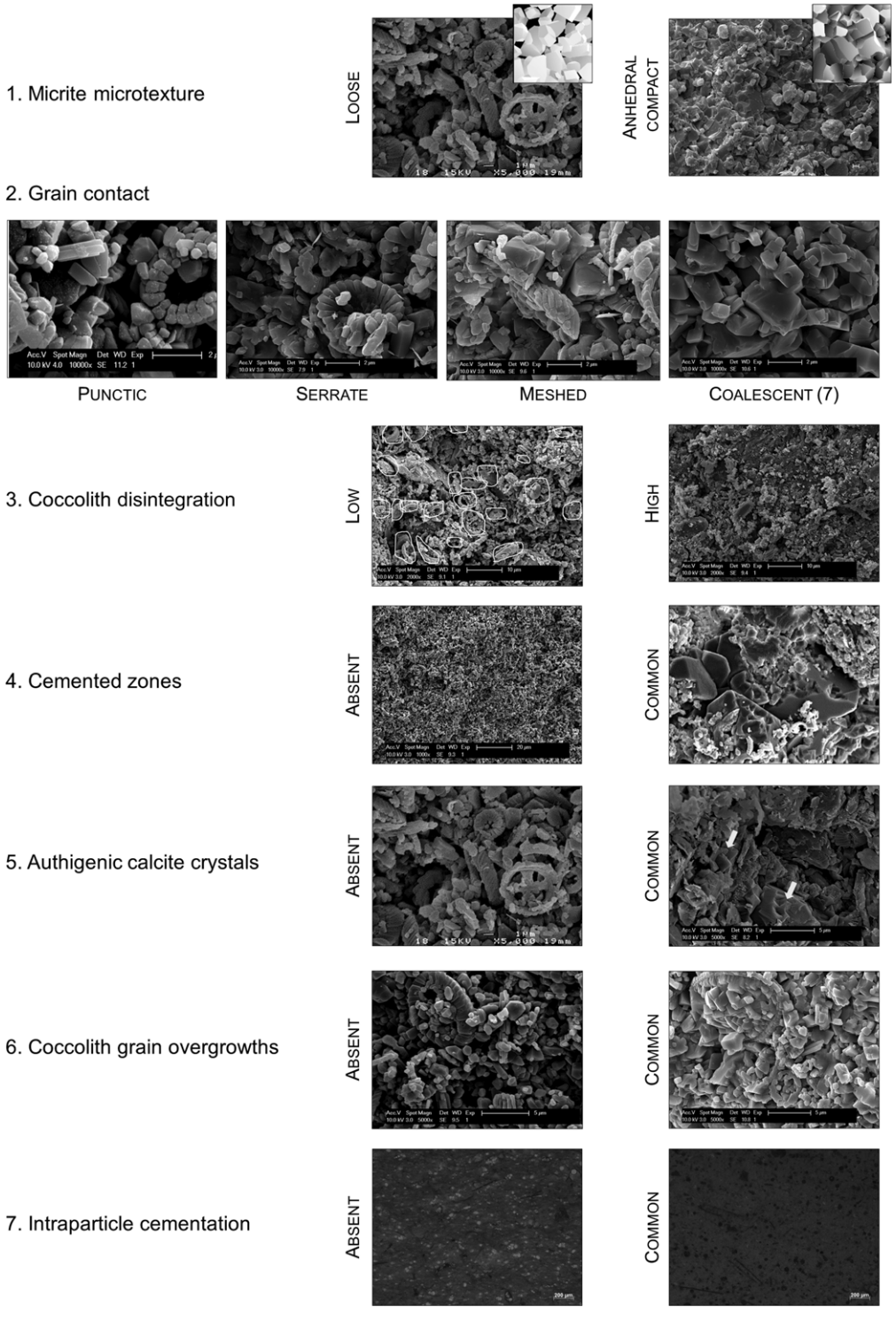

Fig. 3. Typical extreme cases encountered for the seven diagenesis-related criteria. Sketches in Part 1 from Lambert *et al.* (2006).

surfaces (Hjuler & Fabricius 2009). Overgrowths derive from diagenetic processes either by recrystallization or cementation and tend to be more pronounced as the burial depth increases.

Intraparticle calcite cement. The intraparticle cement is characterized from thin section observations under fluorescent light. Intraparticle cementation in chalk essentially refers to the cementation inside forams and calcisphere tests. The cementation of intrafossil porosity indicates active pressure dissolution and thus significant burial depth (Hjuler & Fabricius 2009). This parameter ranges from 0, when there is no intraparticle cementation, to 10, when the whole intraparticle porosity is filled by cement. In this case the cement is often found in the form of large sparitic calcite crystals.

Petrophysical and mechanical properties

The experimental procedure aimed to determine as many properties as possible from the cored plugs available. Therefore non-destructive testing techniques were used to determine the porosity, permeability, dry and saturated P-wave velocities before performing uniaxial compression tests.

Porosity and permeability. Porosity was determined both by water saturation (φ_{water}) and helium expansion (φ_{He}) techniques. In the first method, the void volume was directly measured by a water saturation stage followed by a drying stage; the bulk volume was deduced from the core dimensions. Saturation and drying operations were performed according to American Petroleum Institute (API) standard methods (API 1998). In the second method, a Boyle's law EPS porosimeter was used to determine the grain volume (API 1998). Those porosity measurements correspond to connected pore space.

The gas permeability of the samples was determined with a Vinci nitrogen permeameter. The plugs were mounted in a Hassler-type core-holder at a confining pressure of 28 bar and a steady state gas flow was established through the samples. The permeabilities were corrected for gas slippage using the Klinkenberg empirical correlation (API 1998).

P-wave velocity. Ultrasonic measurement is a non-destructive method used to determine the velocity of ultrasonic waves in materials. Velocity is influenced by the rock type, density, porosity, water content and defects and is therefore closely related to the rock properties (Kahraman 2007). In this study, a PUNDIT Plus system with 54 kHz P-wave transducers was used to determine both the dry and saturated velocities. The velocities were computed from the measured transit time (resolution 0.1 μs) and length (resolution 0.01 mm) of the samples in a pulse transmission arrangement (Rummel & van Heerden 1978). Vaseline was used as the coupling fluid.

Unconfined compressive strength tests. The unconfined compressive strength (UCS) test is a widespread measurement used to mechanically characterize rock materials. The International Society for Rock Mechanics (Fairhurst & Hudson 1999) recommends cylindrical samples with a height to diameter ratio between 2.0 and 3.0. However, smaller height to diameter ratios can also give acceptable results (Dzulinski 1969; Thuro *et al.* 2001). As a result of chalk's very small grain size, smaller samples are still representative. For instance, Duperret *et al.* (2005) used length to diameter ratios ranging from only 1.1 to 1.4. In this study, the tested samples had a length to diameter ratio between 1.2 and 1.6.

Tests were performed on a stiff frame with a servo-controlled loading rate (Fig. 4). Pressure transducers were used to measure the axial stress (range 0–35 MPa or 0–493 MPa depending on the transducer used). Inductive displacement transducers (range ± 1.5 mm) were used to compute the axial strains, leading to a full record of the stress–strain curves. The UCS and Young's modulus (the average modulus of the linear portion of the axial stress–strain curve) could then be computed (Fairhurst & Hudson 1999).

Experimental results

The experimental workflow was applied to 35 samples. Detailed results for the petrographic description are given in Table 1 and the petrophysical and mechanical properties are given in Table 2.

Petrographic results

The dataset acquired covers a wide range of chalks, especially tight chalks, characterized by a spectrum of sedimentary textures, non-carbonate content, various degrees of cementation and compaction. Six lithotypes could be defined based on sedimentary features, colour and apparent strength: micritic, grainy, marl seam, argillaceous, cemented and silicified chalk. However, rather than the lithotype, it is the microtexture (i.e. the description of the arrangement of the matrix micrograins observed under SEM) that is expected to constrain the petrophysical properties of chalk. For each lithotype, a brief description of the associated microtexture is given in the following text. For more details, see Faÿ-Gomord *et al.* (2016*a*), where the impact of microtexture on petrophysical properties is discussed and typical SEM images are shown.

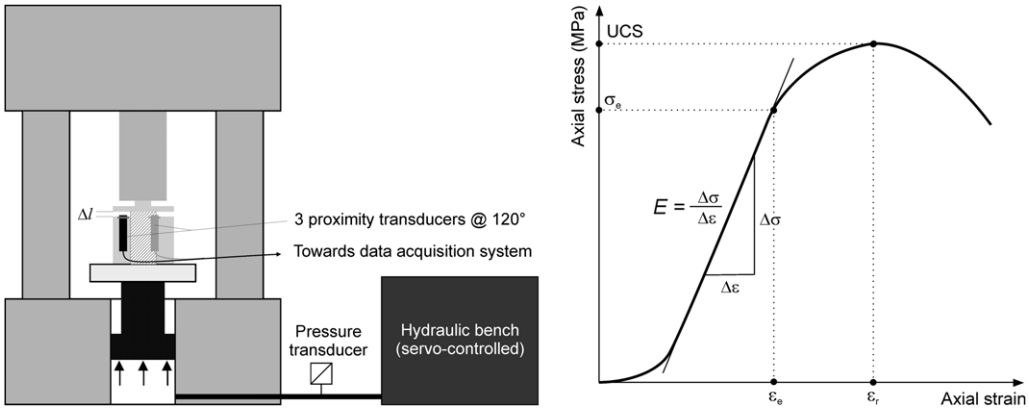

Fig. 4. Sketch of the uniaxial compression test equipment and parameters determined from a typical stress–strain curve.

Micritic chalks have a mud-dominated texture (often mudstone, occasionally wackestone) according to the Dunham (1962) classification. Micritic chalks are mainly composed of coccolith fragments, leading to a micro-rhombic matrix texture, with rare authigenic calcite crystals. Contacts between coccolith fragments are mostly punctic and the interparticle porosity is well preserved.

Grainy chalks are grain-dominated and display a packstone texture. Macroscopically, they cannot always be distinguished from micritic chalks, as they also correspond to pure chalks. However, they show a higher foram and bioclastic content in thin section, giving rise to their packstone texture (Dunham 1962), with 32–43% of grains occurring in a micritic matrix. Under SEM, the micritic matrix of grainy chalks is similar to that of micritic chalk.

Marl seams in chalks are mostly interpreted as the result of pressure solution resulting from burial diagenesis (Lind 1993). Marl seam chalks have a mudstone–wackestone texture, with the percentage of grains ranging from 6 to 17%. Fluorescence microscopy highlights the presence of intraparticle porosity inside calcispheres, forams and various bioclasts. Unlike other chalk lithotypes, there is no one typical texture associated with marl seam chalks. In clay-rich seams, the microtexture is dominated by clay flakes, which may show a preferential orientation. A few millimetres away from the clay seams, the texture is not dominated by the clay content and microtextural features include authigenic cement crystals and grain overgrowths, which do not develop in clay-rich seams. Marl seams seem to develop preferentially in nodular chalk and are affected by early diagenesis and the clays concentrated between the nodules.

Argillaceous chalks are clearly identifiable macroscopically by their light to dark grey colour. They initially formed during the Cenomanian stage where specific sedimentological conditions occurred (with a great detrital input, as described by Deconinck & Chamley 1995; Faÿ-Gomord *et al.* 2016*a*), leading to petrographic characteristics somewhere between those of marls and chalk. Thin section observations show that the clays are dispersed in a brownish matrix. The texture of argillaceous chalk varies from mudstone to wackestone, where the grains mostly include forams, bioclasts and calcispheres. Under SEM, argillaceous chalks are easy to identify, with clay flakes dispersed in the matrix; mechanical compaction tends to align the flakes on a parallel plane to the bedding.

Cemented chalks exhibit a mudstone texture, with 5–8% grain content, and the grains are either cemented with sparite crystals or are micritic. All cemented chalks show similar microtextures with coalescent grain contacts, many authigenic calcite crystals and grain overgrowths. Deeply buried chalks show a higher disintegration of coccoliths and seemingly more grain overgrowths than early cemented chalks.

Outcrops of silicified chalk are scarce, but these chalks have been described in the Ekofisk and South Arne oilfields in the North Sea (Jakobsen *et al.* 2000; Lindgreen *et al*. 2010; Gennaro *et al.* 2013). Only one sample of silicified chalk was investigated in this study, from a 30 cm thick bed from Brunneval (Normandy, France). The rock still had a chalk texture with distinct bioclasts, but its strength was increased compared with the surrounding chalk. Patches of amorphous silica were present in higher porosity zones, whereas lower porosity zones appeared completely silicified, with chalcedony within what used to be the chalk matrix.

Table 2. *Petrophysical and mechanical properties*

Lithotype	Sample no.	Diagenetic index	φ_{water} (%)	φ_{He} (%)	k (mD)	Grain density ($g \cdot cm^{-3}$)	$V_{P\ dry}$ ($m\ s^{-1}$)	$V_{P\ sat}$ ($m\ s^{-1}$)	UCS (MPa)	E (MPa)
Micritic	CH01	1	44.14	41.90	3.18	2.70	2742	3298	7	9469
	CH02	0.5	43.01	44.60	4.48	2.71	2434	2921	4	1224
	CH04	0.5	41.38	42.40	2.85	2.71	2563	2919	5	–
	CO01	1	42.31	42.90	5.83	2.70	2873	2924	5	2585
	NH03	2.5	26.69	28.50	1.84	2.71	4931	4256	–	–
	RA01	1.5	–	45.90	5.95	2.70	2594	2541	4	1187
Grainy	BG01	1	–	37.80	3.09	2.68	2704	2961	5	5455
	CM02	1	39.18	39.70	3.67	2.70	3525	3550	8	9607
	CM06	1	42.41	43.60	4.32	2.71	2602	2728	4	358
	ETR33	2	30.48	33.80	13.30	2.70	2813	2966	3	1068
	SS01	1.5	36.65	40.20	3.10	2.68	2930	2723	4	1345
Argillaceous	CB02	3	26.4	21.60	0.10	2.69	3544	2154	–	–
	CB04	4	–	18.80	0.06	2.69	3544	3111	–	–
	CB06	3.5	–	23.40	0.11	2.68	3095	2476	20	40 542
	CB07	5.5	20.96	21.40	0.13	2.70	4752	4265	21	53 062
	CB09	4	24.09	22.10	0.08	2.68	4310	3012	29	22 442
	CB10	6	23.83	18.90	0.10	2.70	3553	2481	24	35 799
	CB11	3.5	–	23.80	0.10	2.69	4797	2863	–	–
	CB23	5	23.29	21.00	0.06	2.68	3976	2806	27	–
	CB24	3.5	19.03	18.20	0.08	2.67	4536	3724	24	26 401
	CB25	4	22.34	20.10	0.06	2.69	3795	2753	–	–
	EA01	5	15.39	14.20	0.06	2.72	4762	3788	–	–
Marl seam	CB13	3	32.85	31.40	0.30	2.68	3696	2343	15	2674
	CB16	4.5	23.68	20.70	0.19	2.71	4107	3739	–	–
	EA02	5	16.86	14.50	0.25	2.70	5618	4274	24	38 958
	ETR21	1	36.37	36.40	1.32	2.70	3494	3269	12	7855
	ETR47	1.5	38.94	40.40	2.68	2.68	2964	2592	10	–
	SC02	3.5	33.03	33.00	0.48	2.68	3229	2447	–	–
	SC03	3	24.62	25.40	0.40	2.69	4630	3788	19	14 090
Cemented	CB14	6.5	26.89	27.10	0.43	2.70	4090	3514	20	–
	FA15	6.5	15.81	17.60	0.10	2.71	7232	6653	20	50 789
	FA39B	7	15.20	16.20	0.14	2.71	6944	6716	30	23 444
	FH11	7.5	15.98	19.30	0.16	2.71	6526	6200	31	41 935
	SC01	6	23.69	23.80	0.44	2.70	5208	4673	21	23 021
Silicified	BR01	8	26.21	26.40	0.04	2.45	4550	4960	51	25 076

E, Young's modulus; k, empirical Klinkenberg permeability; UCS, unconfined compressive strength; $V_{P\ dry}$, dry P-wave velocity; $V_{P\ sat}$, saturated P-wave velocity; φ_{water}, water saturation porosity; φ_{He}, helium porosity.

Petrophysical and mechanical results

As shown in Figure 5, the porosity determined either by water saturation or helium porosimetry gave very similar values, ranging between 14 and 46%. The porosity in marl seam chalk ranged between 14 and 40% due to variations in the intensity of compaction in those rocks.

The measured permeabilities ranged between 0.04 and 13 mD. Following the definition of the JCR group, we defined tight chalks as having a matrix permeability <0.2 mD (Bailey *et al.* 1999) and therefore almost half of the samples tested in this study (16/35) can be considered as tight chalks based on this criterion. All the argillaceous chalk samples were tight, as well as the deeply buried cemented chalk samples from Flamborough Head (UK samples FA15, FA39 and FA11), the nodular marl seam chalk sample from the base of the Turonian at Cap Blanc Nez (CB16) and the silicified chalk sample (BR01). As the permeabilities are low, fracture porosity is absent and the porosity is associated with interparticle voids. Therefore the measured connected porosity can be considered as the total porosity.

Mercury injection capillary pressure measurements were performed on the same samples. They showed pore throat diameters ranging from 25 to 1100 nm (Faÿ-Gomord *et al.* 2016*a*). The largest pores were found in micritic (510 nm) and

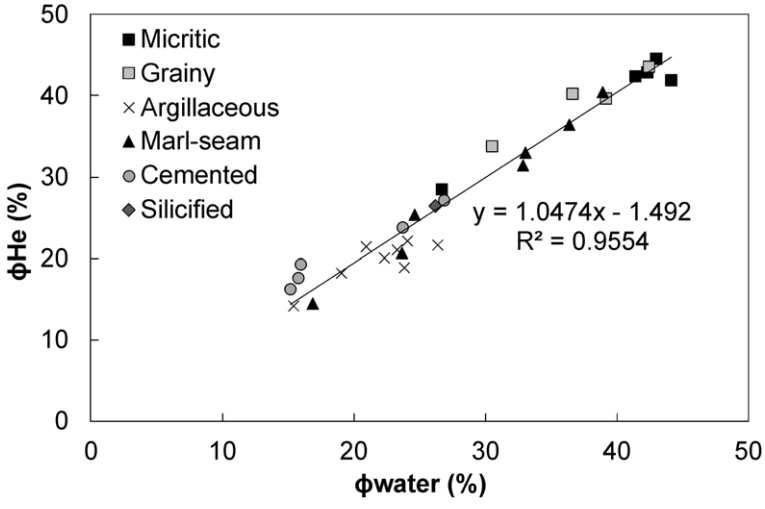

Fig. 5. Correlation between water and helium porosities.

grainy chalk (760 nm), whereas the smallest pores occurred in argillaceous (100 nm) and silicified chalk (25 nm). The pore size distribution was generally unimodal.

UCS tests were performed on dry samples. Despite the variety of sedimentary and diagenetic systems investigated in this study, the mechanical behaviour of chalk under atmospheric conditions was generally characterized by brittle failure. A wide range of values for the UCS was observed, from a few MPa for micritic and grainy chalks to several tens of MPa for argillaceous, cemented and silicified chalks (Fig. 6). The computed Young's moduli varied between 350 and 53 000 MPa. The upper limit may seem high, but the type of chalk investigated in this work can be very different from traditional pure chalk. In some cases, plastification was observed before failure, mainly in the grainy and argillaceous chalks.

Discussion

This study investigated the impact of diagenesis on the petrophysical and mechanical properties of chalk. This will contribute to our understanding of the effect of diagenesis on the storage capacity, transport mechanisms and mechanical behaviour of tight chalk formations. It may also be helpful for identifying outcrop analogues. The following discussion focuses first on the typical diagenetic indices associated with the six lithotypes. The relationships between the petrophysical and mechanical properties are then investigated and related to diagenetic considerations and lithotypes.

Overview of lithotypes and associated diagenesis index

Six lithotypes were identified within the dataset: micritic, grainy, marl seam, argillaceous, cemented and silicified chalks. They were associated with typical ranges of the diagenesis index. The lowest diagenesis indices (<2.5) correspond to micritic and grainy chalks. The loose matrix texture, punctic contacts between grains, rare authigenic calcite crystals, a lack of coccolith grain overgrowth and intraparticle cementation encountered in these microtextures showed the limited cementation of the chalks.

The marl seam chalks exhibited a wider range of diagenesis indices (1–5) because of their heterogeneous nature (clay seams and surrounding chalk). SEM observations indicated a wide range of microtextures relating to the intensity of the burial pressure solution or the initial sedimentary clay content.

The highest diagenesis indices were found in argillaceous, cemented and silicified chalks. In the argillaceous chalks the contacts between coccolith fragments were reduced and very limited grain-to-grain contact dissolution or grain overgrowths developed as a result of the dispersed clay flakes in the matrix. The matrix appeared to be more compact in the argillaceous chalks than in the micritic chalks as a result of compaction by clay-rich chalks, resulting in tighter particles with a higher degree of coccolith disintegration. In the cemented chalks, the high diagenesis index can be explained by the coalescence of grain contacts, the development of many authigenic calcite crystals and grain overgrowths. For the silicified chalk

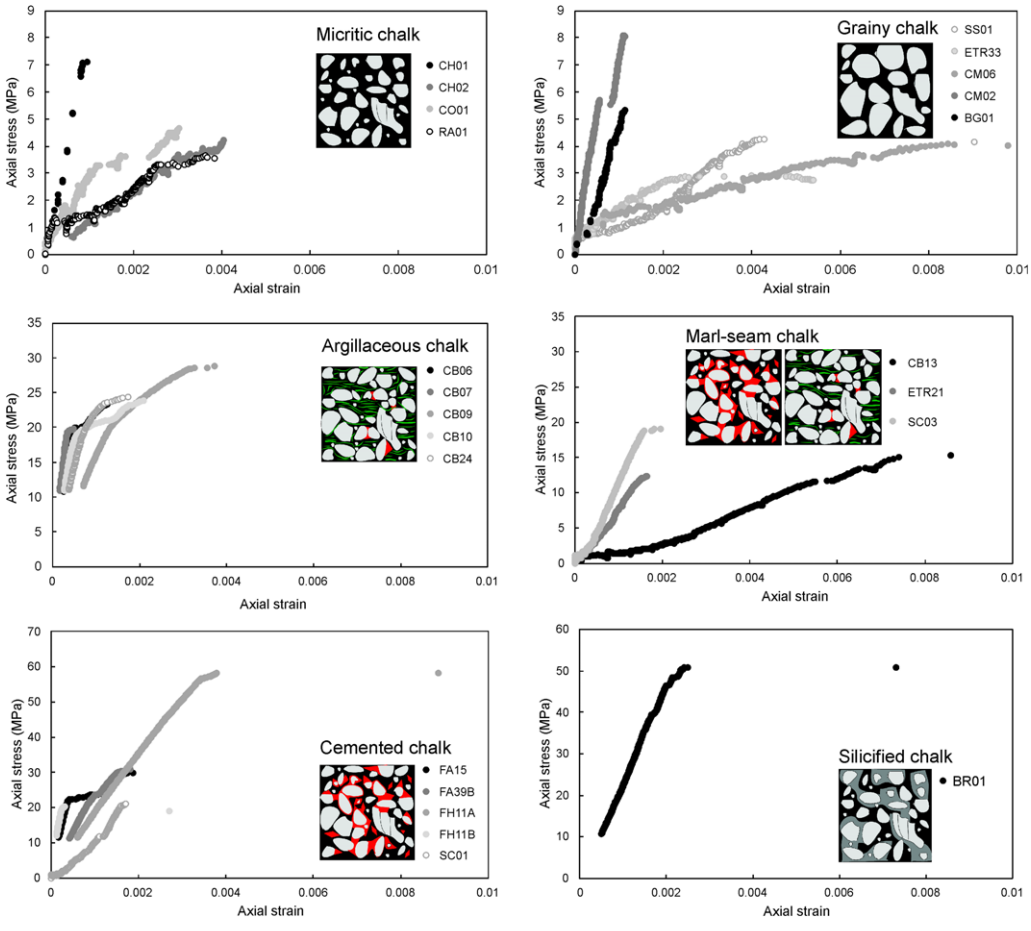

Fig. 6. Uniaxial compression curves for the various lithotypes. The sketches show the typical microtexture(s) associated with each lithotype.

sample, the insoluble residue increased to 76%, with silica dispersed in the chalk matrix and developed as a cement in forams and calcisphere chambers.

Relationships between petrophysical and mechanical properties

Porosity–permeability relationships are often considered in petrophysical studies, particularly to establish correlations within one given formation (Tiab & Donaldson 2004). The relationship is not straightforward because high-porosity rocks may show very low permeabilities and highly permeable rocks may have a low porosity. Among the studied samples, covering a wide range of chalk microtextures, the porosity and the logarithm of the permeability followed a linear relationship (Fig. 7a). The defined microtextures corresponded to typical areas within the cross-plot: micritic and grainy chalks showed the highest porosities and permeabilities, whereas argillaceous, cemented and silicified chalks were less porous ($<30\%$) and less permeable (<1 mD). The porosity–permeability values are related to the intensity of the diagenetic processes because the highest porosities and permeabilities are associated with the lowest diagenesis indices. Figure 7a also compares the data with porosity–permeability values in the JCR database. These data are from North Sea chalks (the Tor, Hod and Ekofisk formations) and their analogues. They are generally in good agreement with our values, although there is more scatter in the JCR data.

The P-wave velocities of both the dry and saturated samples ranged between 2 and 7 km s^{-1} (Fig. 7b). The saturated P-wave velocities were generally higher than the corresponding dry values in the micritic, grainy and silicified chalks; water filled

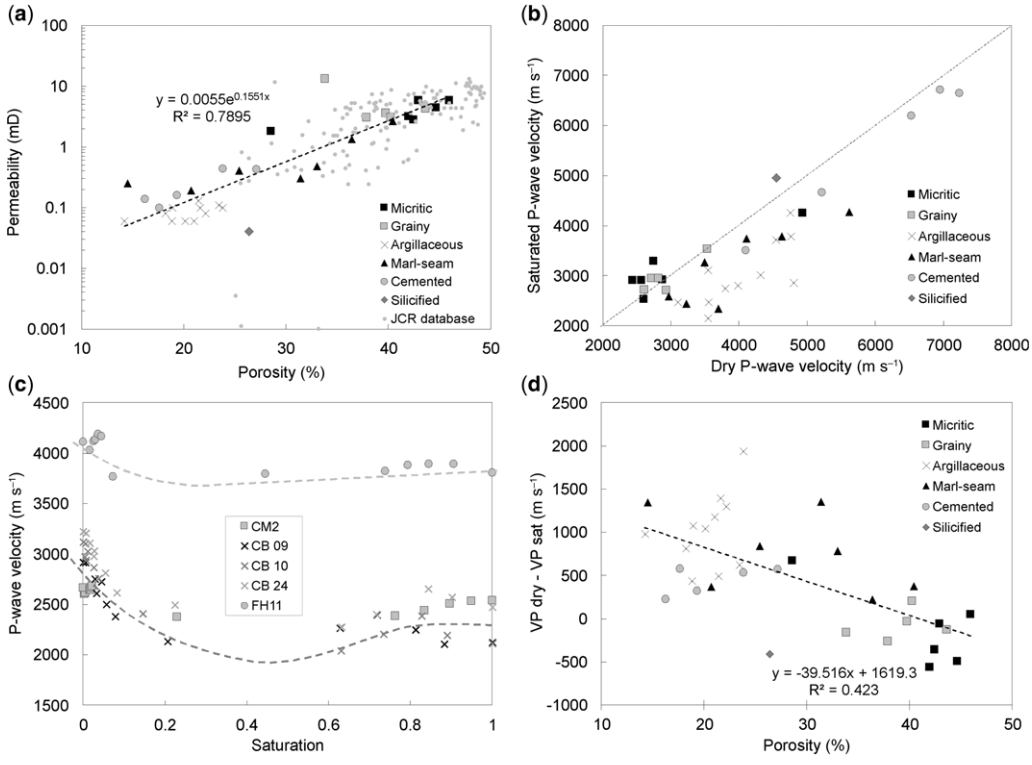

Fig. 7. (**a**) Porosity–permeability plot of data from this study classified by lithotype and comparison with porosity–permeability data from the JCR database. (**b**) P-wave velocities measured on saturated and dry samples. (**c**) P-wave velocity v. saturation plot. CM2 is a grainy chalk; CB09, CB10 and CB24 are argillaceous chalks. FH11 is a cemented chalk. (**d**) Relationship between dry and saturated P-wave velocities and porosity.

voids are more difficult to compress than air-filled voids and tend to increase the P-wave velocities (Bourbié *et al.* 1986).

However, for almost half of the samples, the dry P-wave velocities were higher than the velocities in the saturated samples; this mainly occurred in the argillaceous and marl seam chalks, but also in cemented chalks. To better understand the physical mechanism for this, the P-wave velocity was measured at various saturation values for several samples. Figure 7c shows that the velocity was at a maximum for dry rocks and rapidly decreased for a small water saturation. At high saturation states, the P-wave velocity stabilized or slightly increased, but did not reach the value of the dry material. The introduction of water to a dry sample first increases its density, resulting in a decrease in the velocity (Gassmann 1976; Bourbié *et al.* 1986). With increasing saturation, the apparent rigidity of the material decreases as well as the velocity. Beyond a limit of saturation, water compressibility is important and tends to harden the material, as predicted by Gassmann (1976).

The evolution of P-wave velocity with fluid saturation has already been observed for pure chalk (Schroeder 2002), emphasizing a minimum velocity at partial saturation. In that case, the dry velocities were lower than the fully saturated velocities. Murphy (1982) observed higher dry velocities for the Massillon sandstone (23% porosity). The presence of clay minerals may explain the difference between dry and saturated P-wave velocities. Longitudinal waves show lower velocities in dry clays than in saturated clays. Ghorbani *et al.* (2009) have shown a desiccation-driven hardening when measuring the elastic wave velocities of clay rocks.

As clay minerals were not found in all the samples, other parameters were also investigated. A point to consider is the relationship between P-wave velocities and porosity. Gregory (1976) proposed three characteristic behaviours for the P-wave velocity–saturation relationship of consolidated sediments depending on their porosity. Low porosity sediments ($<10\%$) exhibit dry P-wave velocities that are much smaller than the saturated velocities, with a sigmoidal evolution. For medium

(10–25%) to high-porosity sediments (>25%), the P-wave velocity decreases when a small amount of water is introduced; the decrease is steeper for more porous sediments. An increase in velocity at higher saturation levels is also observed and linked to the compressibility of the fluid. Gregory (1976) observed that the difference between dry and saturated P-wave velocities depends on the porosity, but did not propose a mathematical relationship. For the chalk samples tested in this study, Figure 7d also suggests a relationship between porosity and the difference between dry and saturated P-wave velocities. A linear correlation was attempted, but the complexity of the chalks produced scatter in the data ($R^2 = 0.423$).

In terms of mechanical behaviour, a linear relationship is generally considered to show the influence of porosity (or intact dry density) on UCS (Mortimore & Fielding 1990; Duperret *et al.* 2005). This study confirmed a correlation between porosity and UCS (Fig. 8a). However, the data, as well as previously reported data, showed some scatter from the straight correlation line, meaning that porosity alone cannot be considered as the intrinsic parameter governing the mechanical strength of chalk. The mineralogical composition (e.g. silica and clay minerals) also has a non-negligible effect on the mechanical behaviour of chalk (Monjoie *et al.* 1985; Schroeder 2002).

The features observed and rated through the diagenesis index are the result of both eogenetic and mesogenetic processes affecting chalk; they quantify the diagenetic alteration of chalk. During eogenesis, a low sedimentation rate may result in the early formation of indurated surfaces on the seafloor and thus the early cementation of chalky sediments. Later, mesogenetic processes occur during burial diagenesis and lead to the formation of cements, either by grain overgrowth or authigenic calcite crystals in the matrix. Hence the diagenesis index is a means of quantifying cementation, which strengthens grain contacts and increases the UCS (Fig. 8b). This cross-plot indicates a higher correlation coefficient between the UCS and the diagenesis index than between the UCS and porosity. Several factors can reduce porosity, such as the presence of clay minerals, but these factors do not necessarily reinforce the microstructure, whereas cementation

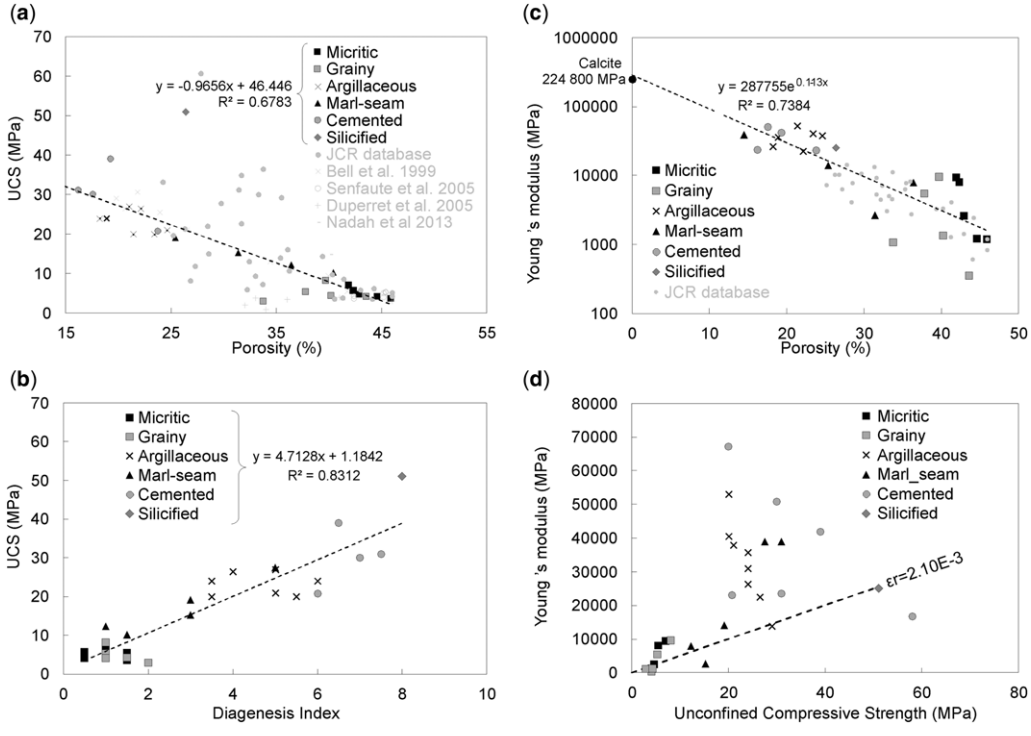

Fig. 8. (**a**) UCS data from this study as a function of porosity, classified by lithotype, and comparison with previously reported UCS–porosity data. (**b**) UCS as a function of diagenesis index. (**c**) Relationship between Young's modulus and porosity, according to lithotype, and comparison with data from the JCR database. (**d**) Relationship between Young's modulus and UCS.

strengthens the mechanical properties of chalk. This result is also important because it emphasizes how features observed at the SEM scale influence mechanical behaviour, whereas the depositional facies, as observed from thin section, only poorly constrain the petrophysical and geomechanical properties (Faÿ-Gomord *et al.* 2016*a*). The microtexture, essentially defined by the non-carbonate content and the degree of diagenesis, controls the mechanical properties of the sample.

The microtextural families were associated with specific mechanical behaviour (Fig. 6). The micritic and grainy chalks underwent less cementation during diagenesis and were the weakest and more deformable materials in the dataset. It has previously been shown that the presence of clays in chalk from deposition enhances chemical compaction (Mallon & Swarbrick 2002, 2008; Fabricius *et al.* 2008). This is why argillaceous chalk has a higher diagenesis index than pure chalk (micritic or grainy) with a similar burial history. Argillaceous chalks are therefore stronger and stiffer than micritic or grainy chalks. In cemented chalk, the coalescence of grain contacts and the development of many authigenic calcite crystals and grain overgrowths explain the high diagenesis index and subsequent high compressive strength. Cementation is controlled by a range of factors; texture, burial history and fluids (Schroeder 2002; Hjuler & Fabricius 2009) can all affect the mechanical properties.

The Young's modulus was found to be an exponential function of porosity (Fig. 8c). The data in this study are in good agreement with values in the JCR database, but cover a wider spectrum of chalk types and properties because the tested material was not limited to reservoir chalks. Engstrøm (1992) used a similar correlation for Danish chalk and proposed an extrapolation towards the Young's modulus of pure calcite (224 800 MPa) for zero porosity:

$$E = 224\,800\, e^{-0.112\varphi} \quad (1)$$

where E is the Young's modulus (MPa) and φ is the porosity. This principle was also applied in this work and gave good results for a wider dataset. Effective media models have been proposed to explain the relations between elastic properties and porosity. The modified upper Hashin–Shtrikman model (Nur *et al.* 1998; Walls *et al.* 1998; Anderson 1999) considers a mixture of hollow spherical shells of one component filling the space, whereas the other component fills the spheres. A first end-member corresponds to zero porosity and the elastic properties are those of the solid phase (mainly calcite); a second end-member depends on a critical porosity estimated to be 50 (Bhakta & Landro 2013) or 70% (Fabricius 2007) for chalk. Fabricius (2003) proposed the iso-frame model, which considers mixtures of suspended solids in the spherical pores of a solid. This modification estimates that not all the grain materials take part in building the frame in the Hashin–Shtrikman model and some will stay in suspension in the pore space. In other words, part of the solid is in suspension in the pore fluid and this suspension is embedded in the supporting frame of calcite and silicates (Fabricius *et al.* 2005).

The relationship between Young's modulus and the UCS was also examined (Fig. 8d). Our results were less clear than previously reported results (Schroeder 2002), which were limited to pure chalk. The idea of a constant brittle failure strain in the shear mode ($\varepsilon_r = 0.002$) seems to be valid for micritic and grainy chalks and some reservoir chalk (JCR database), but argillaceous and cemented chalk are far from this trend. If diagenesis plays a part in the deformability of these chalks, other factors will also affect the deformability, such as the occurrence of clay minerals, pore size and shape (Faÿ-Gomord *et al.* 2016*a*). It can explain the scatter in the cross-plot for argillaceous, marl seam and cemented chalk samples.

Conclusions

Chalk is usually defined as a pure, highly porous and low-permeability carbonate rock. This definition only gives a limited insight into the wide variety of existing chalk materials. Considering the increasing interest in unconventional reservoirs, including tight chalk formations, this study broadens the sedimentary and diagenetic systems investigated and showed how diagenesis can affect the petrophysical and the mechanical properties of chalk by studying the relationships between these properties and the associated microtextures.

Several outcrops in NW Europe were sampled and characterized. The petrographic description included the assessment of a diagenesis index that quantified diagenesis using seven criteria. Each criterion was observed on SEM micrographs of the samples at various scales. Petrophysical and mechanical tests were also conducted, including the determination of porosity, permeability, P-wave velocity and UCS tests.

Six lithotypes were defined: micritic, grainy, marl seam, argillaceous, cemented and silicified chalk. They were characterized by a typical range of values for the diagenesis index. The determined petrophysical and mechanical properties cover a wide range of values, with half of the samples being considered as tight chalks. A linear relationship between

porosity and the logarithm of permeability was obtained. Porosity and permeability are linked with diagenetic processes, with the highest values associated with the lowest diagenetic indices where compaction and cementation are less developed.

P-wave velocity was found to be dependent on the saturation state of the samples with, in some cases, higher values for the dry velocity than for the saturated velocity. This can be explained by a combination of two mechanisms: density increases when water is introduced into a dry sample, but the material hardens when the saturation exceeds a threshold value. The predominant mechanism seems to be influenced by the presence of clay and the porosity of the rock.

From a mechanical point of view, a linear correlation between UCS and porosity was confirmed, even when a wide variety of chalks was considered. However, a much better relationship was found between the UCS and the diagenetic index, which quantified the degree of cementation. Argillaceous chalk, in particular, exhibited a higher diagenetic index than pure chalk (micritic or grainy) with a similar burial history. In other words, as a result of their higher degree of cementation, some clay-rich chalks may be stronger than pure chalks subject to a similar burial history. Young's modulus was exponentially linked with porosity; this can be explained by effective medium models. The stiffer chalk samples were also associated with the highest diagenetic indices. Hence typical behaviours in terms of deformability and strength were observed for the six lithotypes. We therefore showed that diagenetic processes, quantified by means of a newly developed diagenesis index, govern the microtextural features of chalk observed at the SEM scale and, in turn, affect the petrophysical and mechanical properties of these rocks.

The authors acknowledge TOTAL for its financial support as part of a Fractured Tight Chalk project, including the PhD of Ophélie Faÿ-Gomord. Our thanks go to Yves Leroy and Bruno Caline, TOTAL, for support granted throughout this study.

References

Amédro, F. & Robaszynski, F. 2000. Les craies à silex du Turonien supérieur au Santonien du Boulonnais (France) au regard de la stratigraphie événementielle. Comparaison avec le Kent (U.K.). *Géologie de la France*, **4**, 39–56.

Amédro, F. & Robaszynski, F. 2001. Les craies cénomaniennes du Cap Blanc-Nez (France) au regard de la stratigraphie évènementielle. Extension géographique de niveaux repères du bassin anglo-parisien (Boulonnais, Kent, Normandie) à l'Allemagne du Nord. *Bulletin Trimestrial la société géologique Normandie Amis Muséum du Havre*, **87**, 9–29.

Anderskouv, K. & Surlyk, F. 2011. Upper Cretaceous chalk facies and depositional history recorded in the Mona-1 core, Mona Ridge, Danish North Sea. *Geological Survey of Denmark and Greenland Bulletin*, **25**, 3–60.

Anderson, J.K. 1999. The capabilities and challenges of the seismic method in chalk exploration. *In*: Fleet, A.J. & Boldy, S.A.R. (eds) *Petroleum Geology of Northwest Europe. Proceedings of the 5th Conference*. Geological Society, London, 939–947, https://doi.org/10.1144/0050939

API 1998. *Recommended Practices for Core Analysis*. 2nd edn. American Petroleum Institute, Washington DC.

Bailey, H., Gallagher, L. *et al.* 1999. *Joint Chalk Research Phase V: A Joint Chalk Stratigraphic Framework*. Norwegian Petroleum Directorate, Stavanger.

Bell, F.G., Culshaw, M.G. & Cripps, J.C. 1999. A review of selected engineering geological characteristics of English Chalk. *Engineering Geology*, **54**, 237–269, https://doi.org/10.1016/S0013-7952(99)00043-5

Bhakta, T. & Landro, M. 2013. Comparison of different rock physics models for chalk reservoirs. *Proceedings of 10th Biennial International Conference & Exposition*, 23–25 November 2013, Kochi, India, Society of Petroleum Geophysicists (SPG), https://www.spgindia.org/10_biennial_form/P295.pdf

Boulvain, F. & Pingot, J-L. 2012. *Genèse du sous-sol de la Wallonie*. Classe des Sciences, Académie royale de Belgique, Brussels.

Bourbié, T., Coussy, O. & Zinszner, B. 1986. *Acoustique des milieux poreux*. Editions Technip, Paris.

Brigaud, B., Vincent, B. *et al.* 2014. Characterization and origin of permeability-porosity heterogeneity in shallow-marine carbonates: from core scale to 3D reservoir dimension (Middle Jurassic, Paris Basin, France). *Marine and Petroleum Geology*, **57**, 631–651, https://doi.org/10.1016/j.marpetgeo.2014.07.004

Bristow, R., Mortimore, R.N. & Wood, C.J. 1997. Lithostratigraphy for mapping the Chalk of southern England. *Proceedings of the Geologists' Association*, **108**, 293–315.

Cantrell, D.L. & Hagerty, R.M. 1999. Microporosity in Arab Formation carbonates, Saudi Arabia. *GeoArabia*, **4**, 129–154.

Collin, F., Cui, Y.J., Schroeder, C. & Charlier, R. 2002. Mechanical behavior of Lixhe chalk partly saturated by oil and water: experiment and modelling. *International Journal for Numerical and Analytical Methods in Geomechanics*, **26**, 897–924, https://doi.org/10.1002/nag.229

Deconinck, J.F. & Chamley, H. 1995. Diversity of smectite origins in Late Cretaceous sediments; example of chalks from northern France. *Clay Minerals*, **30**, 365–379.

Deconinck, J.F., Amedro, F., Fiolet-Piette, A., Juignet, P., Renard, M. & Robaszynski, F. 1991. Contrôle paléogéographique de la sédimentation argileuse dans le Cénomanien du Boulonnais et du Pays de Caux. *Annales de la Société géologique du Nord*, **1**, 57–66.

DeGennaro, V., Delage, P., Cui, Y.-J., Schroeder, C. & Collin, F. 2003. Time-dependent behavior of oil

reservoir chalk: a multiphase approach. *Soils and Foundations*, **43**, 131–147, https://doi.org/10.3208/sandf.43.4_131

DeGennaro, V., Sorgi, C. & Delage, P. 2005. Air–water interaction and time dependent compressibility of a subterranean quarry chalk. Paper presented at the Symposium Post mining, November 2005, Nancy, France, https://hal.archives-ouvertes.fr/ineris-00972513/document

Delage, P., Schroeder, Ch. & Cui, Y.-J. 1996. Subsidence and capillary effects in chalk. *In*: Barla, G. (ed.) *Proceedings of the Eurock 1996 Conference, Prediction and Performance in Rock Mechanics and Rock Engineering*, 2–5 September 1996, Turin, Italy, Balkema, Rotterdam, 1291–1298.

Deville de Periere, M., Durlet, C., Vennin, E., Lambert, L., Bourillot, R., Caline, B. & Poli, E. 2011. Morphometry of micrite particles in Cretaceous microporous limestones of the Middle East: influence on reservoir properties. *Marine and Petroleum Geology*, **28**, 1727–1750, https://doi.org/10.1016/j.marpetgeo.2011.05.002

Dunham, R.J. 1962. Classification of carbonate rocks according to depositional texture. *In*: Ham, W.E. (ed.) *Classification of Carbonate Rocks--A Symposium*. American Association of Petroleum Geologists Memoirs, **1**, 108–121.

Duperret, A., Taibi, S., Mortimore, R.N. & Daigneault, M. 2005. Effect of groundwater and sea weathering cycles on the strength of chalk rock from unstable coastal cliffs of NW France. *Engineering Geology*, **78**, 321–343, https://doi.org/10.1016/j.enggeo.2005.01.004

Dupuis, C. & Vandycke, S. 1989. Tectonique et karstification profonde: un modèle de subsidence original pour le Bassin de Mons. *Annales de la Société géologique Belgique*, **112**, 479–487.

Dzulinski, M. 1969. L'essai de compression simple des matériaux pierreux. *Memoires CERES (nouvelle Série)*, **28**, 60–78.

Engstrøm, F. 1992. Rock mechanical properties of Danish North Sea Chalk. *In*: Joint Chalk Research Program (ed.) *Proceedings of the 4th North Sea Chalk Symposium*, 21–23 September 1992, Deauville, France.

Fabricius, I.L. 2001. Compaction of microfossil and clay-rich sediments. *Physics and Chemistry of the Earth, Part A: Solid Earth and Geodesy*, **26**, 59–62, https://doi.org/10.1016/S1464-1895(01)00023-0

Fabricius, I.L. 2003. How burial diagenesis of chalk sediments controls sonic velocity and porosity. *American Association of Petroleum Geologists Bulletin*, **87**, 1755–1778.

Fabricius, I.L. 2007. Chalk: composition, diagenesis and physical properties. *Bulletin of the Geological Society of Denmark*, **55**, 97–128.

Fabricius, I.L., Prasad, M. & Olsen, C. 2005. Iso-frame modeling of marly chalk and calcareous shale. Search and Discovery Article **#40151**.

Fabricius, I.L., Gommesen, L., Krogsbøll, A. & Olsen, D. 2008. Chalk porosity and sonic velocity v. burial depth: influence of fluid pressure, hydrocarbons, and mineralogy. *American Association of Petroleum Geologists Bulletin*, **92**, 201–223, https://doi.org/10.1306/10170707077

Fairhurst, C.E. & Hudson, J.A. 1999. Draft ISRM suggested method for the complete stress-strain curve for intact rock in uniaxial compression. *International Journal of Rock Mechanics and Mining Science & Geomechanics Abstracts*, **36**, 279–289.

Faÿ-Gomord, O., Soete, J. *et al.* 2016*a*. New insight into the microtexture of chalks from NMR analysis. *Marine and Petroleum Geology*, **75**, 252–271, https://doi.org/10.1016/j.marpetgeo.2016.04.019

Faÿ-Gomord, O., Descamps, F., Tshibangu, J.-P., Vandycke, S. & Swennen, R. 2016*b*. Unraveling chalk microtextural properties from indentation tests. *Engineering Geology*, **209**, 30–43.

Fritsen, A., Crabtree, B. *et al.* 1996. *Description and Classification of Chalks: North Sea Central Graben, Joint Chalk Research Phase IV*. Norwegian Petroleum Directorate, Stavanger.

Gale, A.S., Kennedy, W.J., *et al.* 2005. Stratigraphy of the Upper Cenomanian–Lower Turonian Chalk succession at Eastbourne, Sussex, UK: ammonites, inoceramid bivalves and stable carbon isotopes. *Cretaceous Research*, **26**, 460–487.

Gassmann, F. 1976. Uber die Elastizität Poröser Medien. *Vierteljahrsschrift der Naturforschenden Gesellschaft in Zürich*, **96**, 1–23.

Gaviglio, P., Bekri, S. *et al.* 2009. Faulting and deformation in Chalk. *Journal of Structural Geology*, **31**, 194–207.

Gennaro, M., Wonham, J.P., Sælen, G., Walgenwitz, F., Caline, B. & Faÿ-Gomord, O. 2013. Characterization of dense zones within the Danian chalks of the Ekofisk Field, Norwegian North Sea. *Petroleum Geoscience*, **19**, 39–64, https://doi.org/10.1144/petgeo2012-013

Ghorbani, A., Zamora, M. & Cosenza, P. 2009. Effects of desiccation on the elastic wave velocities of clay-rocks. *International Journal of Rock Mechanics and Mining Science & Geomechanics Abstracts*, **46**, 1267–1272.

Gommesen, L. & Fabricius, I.L. 2001. Dynamic and static elastic moduli of North Sea and deep sea chalk. *Physics and Chemistry of the Earth, Part A: Solid Earth and Geodesy*, **26**, 63–68, https://doi.org/10.1016/S1464-1895(01)00024-2

Gräfe, K.-U. 1999. Foraminiferal evidence for Cenomanian sequence stratigraphy and palaeoceanography of the Boulonnais (Paris Basin, N-France). *Palaeogeography, Palaeoclimatology, Palaeoecology*, **153**, 41–70.

Gregory, A.R. 1976. Fluid saturation effects on dynamic elastic properties of sedimentary rocks. *Geophysics*, **41**, 895–921.

Hjuler, M.L. & Fabricius, I.L. 2009. Engineering properties of chalk related to diagenetic variations of Upper Cretaceous onshore and offshore chalk in the North Sea area. *Journal of Petroleum Science and Engneering*, **68**, 151–170, https://doi.org/10.1016/j.petrol.2009.06.005

Homand, S. & Shao, J.F. 2000*a*. Mechanical behavior of a porous chalk and effect of saturating fluid. *Mechanics of Cohesive-frictional Materials*, **5**, 583–606, https://doi.org/10.1002/1099-1484(200010)5:7<583::AID-CFM110>3.0.CO;2-J

Homand, S. & Shao, J.F. 2000*b*. Comportement mécanique d'une craie poreuse et effets de l'interaction eau/craie.

Première partie: Résultats expérimentaux. *Oil & Gas Science and Technology – Revue d'IFP*, **55**, 591–598.

Homand, S. & Shao, J.F. 2000*c*. Comportement mécanique d'une craie poreuse et effets de l'interaction eau/craie Deuxième partie : Modélisation numérique. *Oil & Gas Science and Technology – Revue d'IFP*, **55**, 599–609.

Homand, S., Shao, J.F. & Schroeder, C. 1998. Plastic modelling of compressible porous chalk and effect of water injection. Paper SPE-47585-MS, presented at SPE/ISRM Rock Mechanics in Petroleum Engineering Conference, 8–10 July 1998, Trondheim, Norway, https://doi.org/10.2118/47585-MS

Jakobsen, F., Lindgreen, H. & Springer, N. 2000. Precipitation and flocculation of spherical nano-silica in North Sea chalk. *Clay Minerals*, **35**, 175–175, https://doi.org/10.1180/000985500546567

Juignet, P. 1974. *La transgression crétacée sur la bordure orientale du Massif armoricain. Aptien, Albien, Cénomanien de Normandie et du Maine. Le stratotype du Cénomanien*. Thesis, Université de Caen.

Kaczmarek, S.E., Fullmer, S.M. & Hasiuk, F.J. 2015. A universal classification scheme for the microcrystals that host limestone microporosity. *Journal of Sedimentary Research*, **85**, 1197–1212, https://doi.org/10.2110/jsr.2015.79

Kahraman, S. 2007. The correlations between the saturated and dry P-wave velocity of rocks. *Ultrasonics*, **46**, 341–348.

Kennedy, W.J. 1969. The correlation of the Lower Chalk of south-east England. *Proceedings of the Geologists' Association*, **80**, 459–560, https://doi.org/10.1016/S0016-7878(69)80033-7

Kennedy, W.J. & Juignet, P. 1975. Carbonate banks and slump beds in the Upper Cretaceous (Upper Turonian − Santonian) of Haute Normandie, France. *Sedimentology*, **21**, 1–42.

Lambert, L., Durlet, C., Loreau, J.P. & Marnier, G. 2006. Burial dissolution of micrite in Middle East carbonate reservoirs (Jurassic–Cretaceous): keys for recognition and timing. *Marine and Petroleum Geology*, **23**, 79–92, https://doi.org/10.1016/j.marpetgeo.2005.04.003

Lasseur, E., Guillocheau, F., Robin, C., Hanot, F., Vaslet, D., Coueffe, R. & Neraudeau, D. 2009. A relative water-depth model for the Normandy Chalk (Cenomanian–Middle Coniacian, Paris Basin, France) based on facies patterns of metre-scale cycles. *Sedimentary Geology*, **213**, 1–26, https://doi.org/10.1016/j.sedgeo.2008.10.007

Law, A. 1998. Regional uplift in the English Channel: quantification using sonic velocity. *In*: Underhill, J.R. (ed.) *Development and Evolution of the Petroleum Geology of the Wessex Basin*. Geological Society, London, Special Publications, **133**, 187–197, https://doi.org/10.1144/GSL.SP.1998.133.01.08

Lind, I.L. 1993. Stylolites in Chalk from Leg 130 Ontong Java Plateau. *In*: Berger, W.H., Kroenke, J.W. & Mayer, L.A. (eds) *Proceedings of the ODP, Scientific Results*, **130**. Ocean Drilling Program, College Station, TX, 445–451.

Lindgreen, H. & Jakobsen, F. 2012. Marine sedimentation of nano-quartz forming flint in North Sea Danian chalk. *Marine and Petroleum Geology*, **38**, 73–82, https://doi.org/10.1016/j.marpetgeo.2012.08.007

Lindgreen, H., Jakobsen, F. & Springer, N. 2010. Nano-size quartz accumulation in reservoir chalk, Ekofisk Formation, South Arne Field, North Sea. *Clay Minerals*, **45**, 171–182, https://doi.org/10.1180/claymin.2010.045.2.171

Maldonado, A., Batzle, M. & Sonnenberg, S. 2011. Mechanical properties of the Niobrara Formation. Paper presented at the AAPG-RMS 2011 Annual Meeting 25–29 June 2011, Cheyenne, Wyoming, USA, Search and Discovery Article #50465.

Mallon, A.J. & Swarbrick, R.E. 2002. A compaction trend for non-reservoir North Sea Chalk. *Marine and Petroleum Geology*, **19**, 527–539, https://doi.org/10.1016/S0264-8172(02)00027-2

Mallon, A.J. & Swarbrick, R.E. 2008. Diagenetic characteristics of low permeability, non-reservoir chalks from the Central North Sea. *Marine and Petroleum Geology*, **25**, 1097–1108, https://doi.org/10.1016/j.marpetgeo.2007.12.001

Marlière, R. 1949. Le site géologique du Captage d'Hainin-Hautrage (Hainaut). *Annales de la Société géologique de Belgique*, **T73**, B55–B90.

Megawati, M., Madland, M.V. & Hiorth, A. 2015. Mechanical and physical behavior of high-porosity chalks exposed to chemical perturbation. *Journal of Petroleum Science and Engineering*, **133**, 313–327, https://doi.org/10.1016/j.petrol.2015.06.026

Menpes, R.J. & Hillis, R.R. 1996. Determining apparent exhumation from Chalk outcrop samples, Cleveland Basin/East Midlands Shelf. *Geological Magazine*, **133**, 751, https://doi.org/10.1017/S0016756800024596

Mitchell, S.F. 1994. New data on the biostratigraphy of the Flamborough Chalk Formation (Santonian, Upper Cretaceous) between South Landing and Danes Dyke, North Yorkshire. *Proceedings of the Yorkshire Geological Society*, **50**, 113–118, https://doi.org/10.1144/pygs.50.2.113

Monjoie, A., Schroeder, Ch., Halleux, L., Da Silva, F., Debande, G., Detiège, Cl & Poot, B. 1985. Mechanical behaviour of chalks. *In*: Amoco Norway Oil Company (ed.) *Proceedings of the 2nd North Sea Chalk Symposium*, May 1985, Stavanger, Norway.

Mortimore, R. & Pomerol, B. 1997. Upper Cretaceous tectonic phases and end Cretaceous inversion in the Chalk of the Anglo–Paris Basin. *Proceedings of the Geologists' Association*, **108**, 231–255.

Mortimore, R.N. 2011. A Chalk Revolution: what have we done to the Chalk of England? *Proceedings of the Geologists' Association*, **122**, 232–297.

Mortimore, R.N. & Fielding, P.M. 1990. The relationship between texture, density and strength of chalk. *In*: Burland, J.B. (ed.) *Chalk, Proceedings of the International Chalk Symposium, Brighton Polytechnic*, 4–7 September 1989. Thomas Telford, London.

Murphy, W.F., III. 1982. Effects of partial water saturation on attenuation in sandstones. *Journal of the Acoustical Society of America*, **71**, 1458–1468.

Nadah, J., Bignonnet, F., Davy, C.A., Skoczylas, F., Troadec, D. & Bakowski, S. 2013. Microstructure and poro-mechanical performance of Haubourdin chalk. *International Journal of Rock Mechanics and*

Mining Science & Geomechanics Abstracts, **58**, 149–165, https://doi.org/10.1016/j.ijrmms.2012.11.001

Nguyen, H.D., DeGennaro, V., Sorgi, C. & Delage, P. 2008. Experimental and modelling investigation on the behaviour of a partially saturated mine chalk. Paper presented at the Symposium Post-Mining 2008, February 2008, Nancy, France. ASGA, Vandoeuvre-les-Nancy.

Nur, A., Mavko, G., Dvorkin, J. & Galmudi, D. 1998. Critical porosity: a key to relating physical properties to porosity in rocks. *The Leading Edge*, **17**, 357–362.

Papamichos, E., Brignoli, M. & Santarelli, F.J. 1997. An experimental and theoretical study of a partially saturated collapsible rock. *Mechanics of Cohesive-frictional Materials*, **2**, 251–278.

Papamichos, E., Berntsen, A.N., Cerasi, P., Vandycke, S., Baele, J-M. & Fuh, G.F. 2012. Solids production in chalk. *In*: Bobet, A. (ed.) *46th US Rocks Mechanics/Geomechanics Symposium*, 24–27 June 2012, Chicago, IL, USA. American Rock Mechanics Association, ARMA Conference Paper 2012–479.

Pollastro, R.M. 2010. Natural fractures, composition, cyclicity, and diagenesis of the Upper Cretaceous Niobrara Formation, Berthoud Field, Colorado. *The Mountain Geologist*, **47**, 135–149.

Quine, M. & Bosence, D. 1991. Stratal geometries, facies, and sea-floor erosion in Upper Cretaceous Chalk, Normandy, France. *Sedimentology*, **38**, 1113–1152.

Rashid, F., Glover, P.W.J., Lorinczi, P., Collier, R. & Lawrence, J. 2015. Porosity and permeability of tight carbonate reservoir rocks in the north of Iraq. *Journal of Petroleum Science and Engineering*, **133**, 147–151, https://doi.org/10.1016/j.petrol.2015.05.009

Regnet, J.B., Robion, P., David, C., Fortin, J., Brigaud, B. & Yven, B. 2014. Acoustic and reservoir properties of microporous carbonate rocks: implication of micrite particle size and morphology. *Journal of Geophysical Research: Solid Earth*, **120**, 790–811, https://doi.org/10.1002/2014JB011313

Richard, J., Sizun, J.P. & Machhour, L. 2005. Environmental and diagenetic records from a new reference section for the Boreal realm: the Campanian chalk of the Mons basin (Belgium). *Sedimentary Geology*, **178**, 99–111, https://doi.org/10.1016/j.sedgeo.2005.04.001

Risnes, R. 2001. Deformation and yield in high porosity outcrop chalk. *Physics and Chemistry of the Earth, Part A: Solid Earth and Geodesy*, **26**, 53–57.

Risnes, R. & Flaageng, O. 1999. Mechanical properties of chalk with emphasis on chalk-fluid interactions and micromechanical aspects. *Oil & Gas Science and Technology*, **54**, 751–758, https://doi.org/10.2516/ogst:1999063

Risnes, R., Haghighi, H., Korsnes, R.I. & Natvik, O. 2003. Chalk–fluid interactions with glycol and brines. *Tectonophysics*, **370**, 213–226, https://doi.org/10.1016/S0040-1951(03)00187-2

Robaszynski, F. & Amédro, F. 1986. The Cretaceous of the Boulonnais (France) and a comparison with the Cretaceous of Kent (United Kingdom). *Proceedings of the Geologists' Association*, **97**, 171–208.

Robaszynski, F., Gale, A.S., Juignet, P., Amédro, F. & Hardenbol, J. 1998. Sequence stratigraphy in the Upper Cretaceous series of the Anglo-Paris Basin: exemplified by the Cenomanian stage. *In*: Graciansky de, P.-C., Hardenbol, J., Jacquin, T. & Vail, P.R. (eds) *Mesozoic and Cenozoic Sequence Stratigraphy of European Basins*. Society of Economic Paleontologists and Mineralogists, Special Publications, **60**, 363–386.

Robaszynski, F., Dhondt, A. & Jagt, J.W.A. 2001. Cretaceous lithostratigraphic units (Belgium). *Geologica Belgica*, **4**, 121–134.

Røgen, B. & Fabricius, I.L. 2002. Influence of clay and silica on permeability and capillary entry pressure of chalk reservoirs in the North Sea. *Petroleum Geoscience*, **8**, 287–293, https://doi.org/10.1144/petgeo.8.3.287

Rummel, F. & van Heerden, W.L. 1978. Suggested Methods for Determining Sound Velocity. *International Journal of Rock Mechanics and Mining Science & Geomechanics Abstracts*, **15**, 53–58.

Schroeder, C. 1995. Le pore collapse: aspect particulier de l'interaction fluide-squelette dans les craies? *In*: *Proceedings of the Colloque international du Groupement Belge de Mécanique des Roches*. Brussels, 1.1.53–1.1.60.

Schroeder, C. 2002. *Du coccolithe au réservoir pétrolier*. PhD thesis, University of Liège.

Senfaute, G., Amitrano, D., Lenhard, F. & Morel, J. 2005. Etude en laboratoire par méthodes acoustiques de l'endommagement des roches de craie et corrélation avec des résultats in situ. *Revue Française de Géotechnique*, **110**, 9–18.

Strand, S., Hjuler, M.L., Torsvik, R., Pedersen, J.I., Madland, M.V. & Austad, T. 2007. Wettability of chalk: impact of silica, clay content and mechanical properties. *Petroleum Geoscience*, **13**, 69–80, https://doi.org/10.1144/1354-079305-696

Tiab, D. & Donaldson, E.C. 2004. *Petrophysics*. 2nd edn. Gulf Professional Publishing, Houston, TX.

Thuro, K., Plinninger, R.J., Zäh, S. & Schütz, S. 2001. Scale effects in rock strength properties. Part 1: unconfined compressive test and Brazilian test. *In*: Särkkä, P. & Eloranta, P. (eds) *Rock Mechanics – a Challenge for Society*. Taylor & Francis.

Vandycke, S. 2002. Paleostress records in Cretaceous formations in NW Europe: extensional and strike-slip events in relationships with Cretaceous-Tertiary inversion tectonics. *Tectonophysics*, **357**, 119–136.

Vandycke, S., Bergerat, F. & Dupuis, C. 1991. Meso-Cenozoic faulting and inferred paleostresses of the Mons basin (Belgium). *Tectonophysics*, **192**, 261–271.

Vincent, B., Fleury, M., Santerre, Y. & Brigaud, B. 2011. NMR relaxation of neritic carbonates: an integrated petrophysical and petrographical approach. *Journal of Applied Geophysics*, **74**, 38–58, https://doi.org/10.1016/j.jappgeo.2011.03.002

Walls, J., Divorcing, J. & Smith, B.A. 1998. Modeling seismic velocity in Ekofisk chalk. Expanded Abstract presented at the 68th SEG Meeting, Society of Exploration Geophysicists.

Whitham, F. 1993. The stratigraphy of the Upper Cretaceous Flamborough Chalk Formation north of the Humber, north-east England. *Proceedings of the Yorkshire Geological Society*, **49**, 235–258, https://doi.org/10.1144/pygs.49.3.235